Improving the Peel Strength of Amorphous Metal Foil to Aerospace-Grade Structural Adhesive

Rose Roberts[1], Matthew Nichols[1], Elizabeth Kidd[1], Flora Mechentel[2], Giles Dillingham[1]
[1]BTG Labs
Cincinnati, OH, USA
[2]Jet Propulsion Laboratory, California Institute of Technology
Pasadena, CA

ABSTRACT

Amorphous metal applications in aerospace have grown with the continuous improvement of production methods. These bulk metallic glass materials, often produced as a foil, generally exhibit stronger mechanical properties and corrosion resistance compared to crystalline metal. An amorphous metal foil was chosen as the best material for a particular satellite component, bonded in place using an aerospace-grade structural adhesive. However, previous work has shown that amorphous metal foils exhibit poor peel strength when bonded with structural adhesives. This paper discusses the mechanics of peel testing and the inherent limitations imposed by the amorphous metal foil properties; peel strength was maximized within these limitations by optimization of surface preparation techniques until cohesive failure in a thin film of adhesive was obtained as shown by surface analysis. The process was further developed for building satellite components on a larger scale.

Keywords: amorphous metals, peel strength, structural adhesives
Corresponding author: Giles Dillingham

1. INTRODUCTION

Capturing images of planets in nearby solar systems is limited due to excess light from the system's central star washing out the image. In order to view distant planets, the Jet Propulsion Laboratory (JPL) is developing a large flower-like structure to block light from a star that would otherwise prevent viewing of the orbiting planets called Starshade [1]. To maximize the Starshade's effectiveness, the shape of the optical edge must be tightly controlled in order to prevent light diffraction around the structure [1]. Certain amorphous metal (AM) alloys can be etched more precisely than crystalline metals such that less light is scattered [2]. The lack of grains in AMs also work to inhibit corrosion and provide generally higher strengths compared with crystalline metals [3,4]. Thus, a particular AM was chosen by JPL due to excellent mechanical and optical performance.

The design of the Starshade's optical edge limits assembly to adhesive bonding. However, these thin metal foils exhibit low peel strength compared with expected values provided by the adhesive manufacturer. In previous work, certain variables as to the cause of poor peel strength were eliminated, including surface cleanliness and surface energy, roughness, metallurgical composition, and crystallinity. The same work also found that peel strength was improved by using a more flexible adhesive or a flexible primer was added during assembly [5]. This suggested that mechanical stress distribution rather than chemistry may be the major cause of low peel strengths.

The effect of flexible peel arm stiffness on peel strength has been previously discussed [6,7]. It has been found that thinner materials with high yield strengths concentrate all load to an extremely small region at the bond line. At this location, the high amount of stress experienced by the system will either plastically deform the peel arm, break the adhesive bond, or both [6,7]. For amorphous metals with high yield strengths, it is most likely that the latter of these scenarios will occur. Additionally, due to the nature of AM production, foil thicknesses are limited to 0.038–0.075 (1.5–3 mil), causing further stress transfer compared with thicker substrates.

Several models have been made to predict peel strength. For example, Bikerman et al. determined that the peel strength of an adherend bonded with an adhesive identified as a Hookean solid, assuming all the force from peeling would be dispersed into the adhesive, could be predicted from the elastic modulus of the adhesive and the thickness of the peel substrate [8]. A more complex model proposed by Kaelble also included peel angle and strain rate to model peel behavior [9]. For this work, the simpler Bikerman model was used as a general comparison of curve shape to generally estimate peel strengths based on data collected.

The purpose of this work was to confirm the theory that mechanical stresses were the cause of low peel strength and to establish an expected upper limit for peel performance. Additionally, methods for improving bond strength to meet the needs of the Starshade were explored, including surface preparation and a primer.

2. EXPERIMENTATION

2.1 Materials

2024 T3 aluminum of multiple thicknesses, including 1.63 mm, 0.51 mm, 0.25 mm, 0.15 mm, and 0.05 mm (0.064, 0.02, 0.01, 0.006, and 0.002 in) was acquired from McMaster-Carr. Amorphous metal MBF 20 was provided by JPL of multiple foil thicknesses, including 0.076 mm, 0.051 mm, and 0.038 mm (0.003, 0.002, and 0.0015 in). Sol gel surface primer (3M™ Surface Pre-treatment AC-130) was acquired from Heatcon. Paste epoxies (LOCTITE® EA 9394 and EA 9360) were purchased from Henkel. Glass beads (0.1 mm) for bondline thickness control were provided by JPL.

2.2 Test Methods

Two materials tests were used to characterize bond performance. The first test was a Lap Shear Tensile test using ASTM D1002 [10]. Aluminum coupons (1.63 mm thick) were bonded to verify the effectiveness of surface preparation by comparing obtained values with those specified in the technical data sheet (TDS) [11,12]. The second test was a Floating Roller Peel Test (ASTM D3167) using multiple thicknesses of aluminum and amorphous metal foils [13]. Peel tests are known to be more sensitive to bond surface quality and relates directly to the stresses experienced by the Starshade assembly in service.

2.2.1 Lap Shear Assembly

Two 2.54 x 10.16 cm (1 x 4 in) coupons of 1.63 mm thick aluminum were adhered using 3.22 cm^2 (0.5 in^2) bond area. Epoxy was manually mixed and spread over the surface with acetone-cleaned

metal spatulas. Bondline thickness was controlled using approximately 0.1% by mass of glass bead spacers to epoxy total mass.

The baseline surface treatment process included solvent wiping (acetone and isopropanol), orbital sanding, and/or alumina grit blasting. Surfaces were clamped together for the duration of the curing process. Excess adhesive squeezed out of the bond area during clamping was scraped off with a spatula prior to initiating the curing process. Curing conditions included 1-hour elevated-temperature cure (ET), 7-day room-temperature cure (RT), and 24-hour room-temperature cure with a 1-hour elevated-temperature post-cure.

2.2.2 Peel Test Coupon Assembly

Peel test coupons were assembled using a rigid substrate consisting of a piece of 8.89 cm x 20.8 cm aluminum sheet of 1.63 mm thickness bonded to a 7.62 cm x 25.9 cm flexible substrate. The thickness of the flexible substrate ranged from 0.51 mm to 0.038 mm. Epoxy was manually mixed and spread over the surface with acetone-cleaned metal spatulas. Bond line thickness was controlled using approximately 0.1% by mass of glass bead spacers to epoxy total mass.

Prior to bonding, surface treatment was applied to the bond surfaces of the rigid and the flexible substrates. Surface preparations that were evaluated include solvent wiping (acetone and isopropanol), orbital sanding, VFN Scotchbrite abrasion, alumina grit blasting, vacuum plasma treatment, and/or sol gel application. Some samples were subjected to multiple surface treatment types. Once panels were mated together, pressure was applied to the flexible substrate with a rubber ink roller to evenly spread the adhesive across both surfaces. The samples were then placed between two 2.54 cm (1 in) thick aluminum platens and pressed together with at least 34.5 kPa (5 psi) of pressure in a hydraulic press. Pressure was maintained for the duration of the cure cycle required to allow the epoxy to become rigid, generally the first 24 hours at room-temperature. Curing conditions included 1-hour ET cure, 7-day RT cure, and 24-hour RT cure with a 1-hour elevated-temperature post-cure. After curing, panels were sectioned into 1.27 cm wide samples, with the outermost edges being cut away and disposed.

2.2.3 Mechanical Testing

Test coupons were evaluated using an Instron Tensile Tester calibrated to ASTM standard E4-20 [14]. Lap shear specimens were tested in accordance with ASTM D1002 using a 2300 kg (5000 lb) load cell and clamping jaw fixtures [10]. Peel test coupons were tested in accordance with ASTM D3167 with a 1 kg (200 lb) load cell, a clamping jaw fixture, and a rolling 45° peel test fixture [13].

2.2.4 Infrared Spectroscopy

Fourier Transform Infrared Spectroscopy (FTIR) was conducted using a Thermo Scientific Nicolet spectrometer with a grazing angle reflection accessory (Harrick Scientific).

3. RESULTS AND DISCUSSION

3.1 Identification of Adhesive Cure Schedule using Lap Shear

Several cure schedules were explored for EA 9394 and EA 9360 to maximize the strength of adhesive joints. The manufacturer's technical data sheets [11, 12] provide ranges of temperatures and times at which the adhesives can be cured, however there is no indication of the effect on adhesive performance.

Previous work by JPL identified transition temperatures during curing of both adhesives at temperatures between the minimum and maximum cure temperatures (data not shown). Since amine cured epoxies can have competing reactions that change crosslinking percentage and chain lengths, the effect of this transition temperature mid-range was explored [15, 16].

Since it is difficult to source small batches of BR-127 coated phosphoric acid anodized (PAA) aluminum, several other surface preparation methods were explored in order to attempt to replicate the TDS values for lap shear and peel strength. Solvent wiping, abrasion, and grit blasting were compared. Lap shear specimens assembled using a grit blasted surface were able to achieve strengths similar to those provided in the TDS. Therefore, lap shear data for grit blasted surfaces only are shown.

Elevated-temperature cures (60 °C, 1 hr) produced higher strength lap shear bonds with a more homogenous failure line for EA 9394, matching the expected TDS values. Comparatively, seven-day room-temperature cure and seven-day room-temperature plus post cure at 108 °C at 1 hr showed decreased lap shear strengths and inhomogeneous fracture surface for EA 9394. At the same conditions, EA 9360 did not show a significant difference in lap shear strengths and also exhibited more homogenous fracture surfaces (Figures 1 and 2).

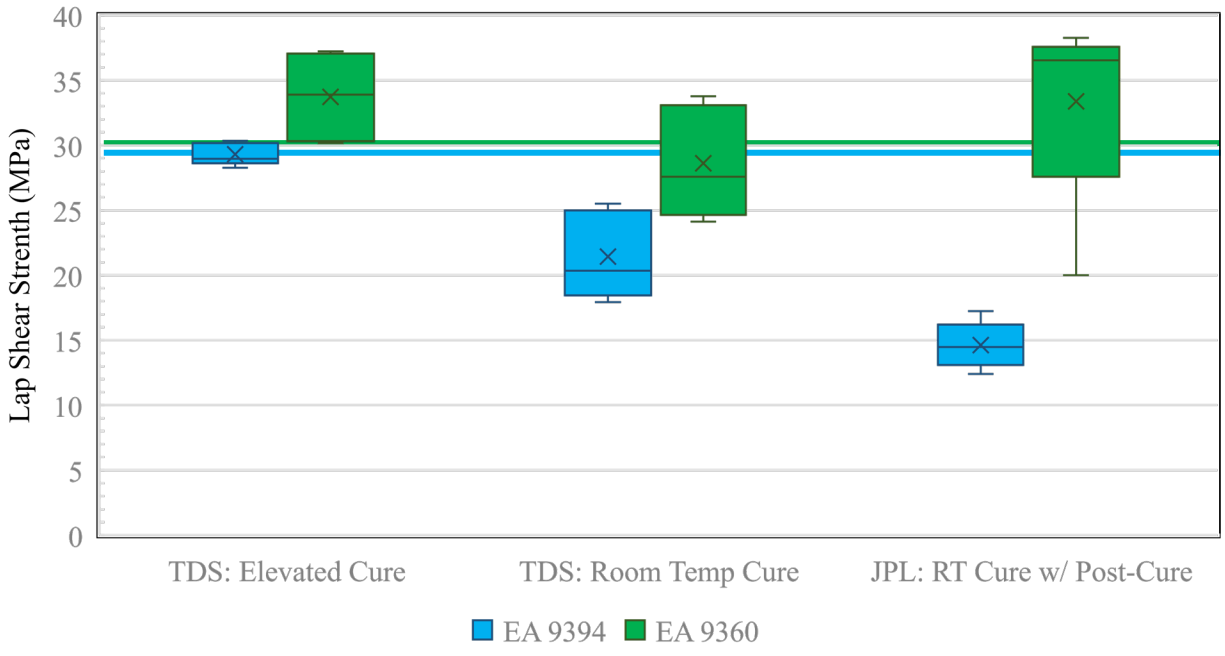

Figure 1. Effect of cure cycle on fracture strength of lap shear joints. TDS expected values are represented by the blue line for EA 9394 and the green line for EA 9360.

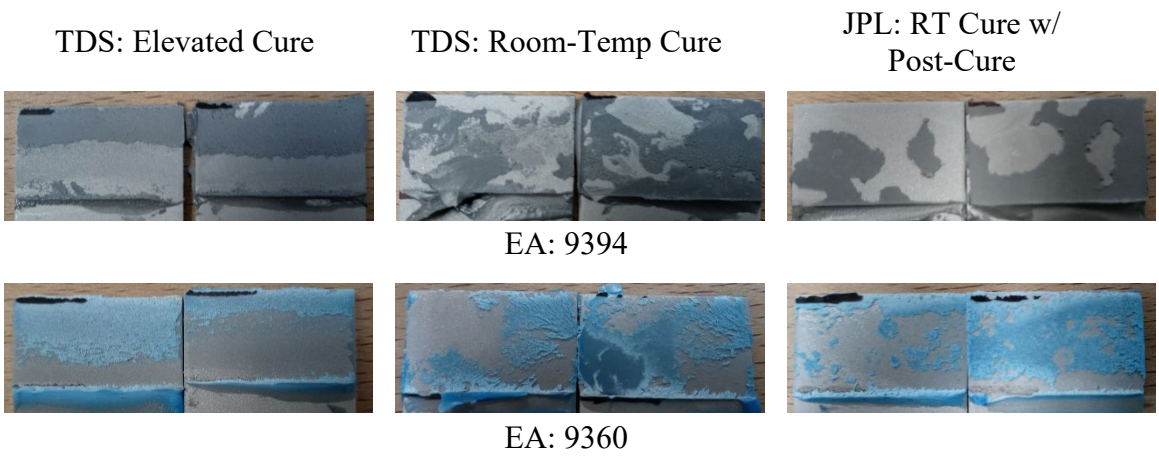

Figure 2. Effect of cure cycle on failure mode of lap shear joints.

3.2 Peel Strength using Lap Shear Surface Preparation Method

Since TDS values of lap shear strength were achieved, the surface preparation methodology was assumed to be sufficient and peel specimens were prepared and assembled in a similar manner using aluminum for both the rigid substrate and the peel arm. However, peel strength showed significantly lower values than provided by the TDS for both adhesives.

Failure mode was monitored visually and confirmed spectroscopically using FTIR (Figure 3). Failure mode was nearly 100% interfacial for EA 9394, with a room-temperature cure exhibiting the least amount of interfacial failure. EA 9360 exhibited nearly 100% cohesive failure for all cure cycles.

Further analysis of peak intensities in FTIR show differences in completion of epoxy curing at different cure temperatures, which is consistent with literature [15,16]. The area under the absorbance peak at 912 cm^{-1}, representing reactive epoxy groups, can be compared with the area under the absorbance peak at 1505 cm^{-1}, representing phenyl rings, to infer epoxy curing completion (Figure 4). Part A of each adhesive type contains the base resin material, including the epoxy groups, while Part B of adhesives contain the amine curing agents. The ratio of epoxide to phenyl rings in Part A of EA 9360 begins as slightly larger than the ratio of EA 9394. By having more epoxy groups, EA 9360 can theoretically achieve a higher crosslink density upon curing, which could lead to better high temperature performance. With a room-temperature cure, the differences in ratios of epoxide to phenyl groups is similar between the two adhesive types. However, with an elevated-temperature cure, the ratios between the two adhesives are similar and the amount of overall reactive epoxy has greatly decreased. This would indicate that a room-temperature cure has not fully reacted and cured.

Amine cured epoxies have shown similar behavior previously [15,16]. The competitive elements of kinetics and diffusion of unreacted species are theorized to be a cause of this phenomenon. At higher temperatures, it is easier for unreacted species to diffuse through the bulk material and find unreacted amine curing agents. This generally leads to a higher percentage of reaction completion compared with lower temperatures, where diffusion becomes more difficult. Reaction completion

and amount of crosslinking affects the mechanical properties of the adhesive and thereby the adhesive's ability to distribute stress under load.

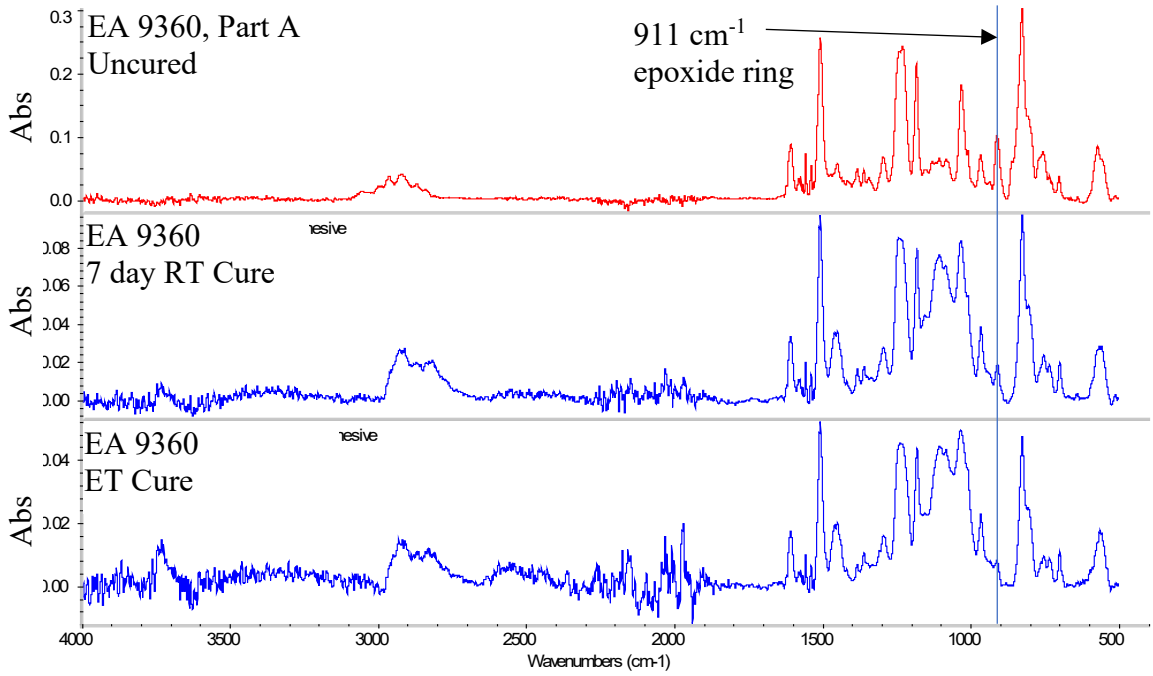

Figure 3. FTIR peak areas decrease in intensity, indicating differences in completion of epoxy adhesive curing.

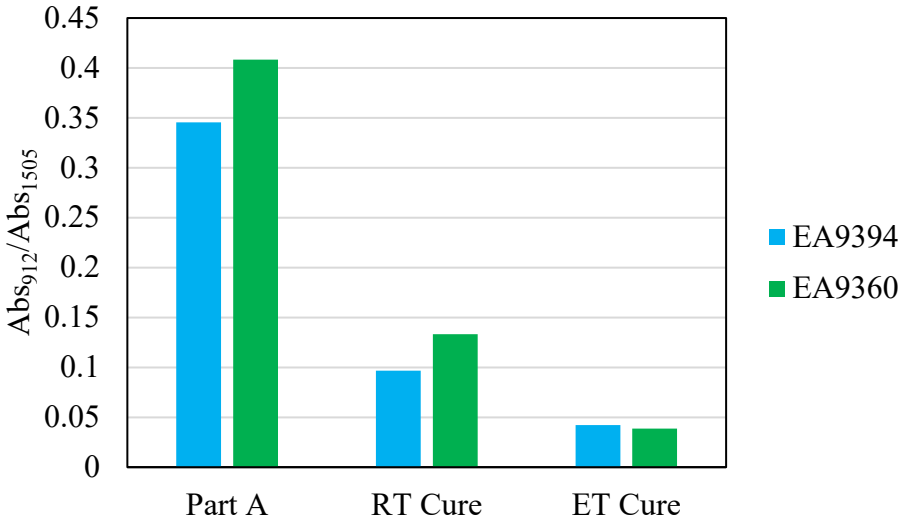

Figure 4. Ratio of FTIR absorbance peaks areas at the reactive epoxide (912 cm^{-1}) and phenyl ring (1505 cm^{-1}). joints.

3.3 Effect of Sol-gel Coating on Peel Strength

Grit blasted samples achieved TDS values for lap shear strength but were extremely low compared with TDS peel values. This is likely due to the differences in surface preparation. TDS peel values were generated from aluminum that was treated with PAA and primed with BR-127. While not yet confirmed, it is theorized that the additional BR-127 coating may provide some additional dispersion of stresses experienced at the local peeling region, thereby increasing the total load the materials system can experience before failure.

A report from the Air Force Research Laboratory compared the effects of sol-gel primer AC-130, BR-127/PAA, and a mild abrasion of aluminum surfaces on peel strengths [17]. Sol-gel primer treated surfaces exhibited similar peel strengths compared with BR-127/PAA surfaces. Both were still significantly lower than TDS reported values, however the strengths were much greater than values achieved on grit blasted surfaces in this work. Sol-gel is a much more practical coating to use for JPL purposes compared with PAA and BR-127, and was thus explored as an additional treatment to improve peel strengths.

Aluminum surfaces were briefly abraded and coated with sol-gel before bonding using EA 9394 and EA 9360. It was found that the sol-gel increased peel strengths by 300-400% compared with a grit blasted aluminum surface and were approaching values achieved by the AFRL report (Table 1). Using a grit blast or hand abrasion before applying the sol-gel both seemed to exhibit similar peel strengths.

Table 1. Comparison of peel strengths (kN/m) of surface treatments and cure conditions for EA 9360 on aluminum substrates.

	TDS[10]	**AFRL[13]**	**BTG Labs**		
	PAA + BR127	**Abrade + sol-gel**	**Grit blast**	**Grit blast + sol gel**	**Abrade + sol gel**
Elevated-Temp Cure	5.25 (65 °C/1 hr)	4.03 (82 °C/70 min)	1.31-1.40 (85 °C/1 hr)	--	--
7 day RT Cure	8.58	--	1.40-2.80	6.65-8.76	--
24 hr RT + 1 hr/85°C	--	--	1.75-2.80	5.60-6.30	5.95-6.65

3.4 Effect of Substrate Thickness on Peel Strength of Aluminum

The effect of aluminum peel substrate thickness on peel strength was also explored and compared with the Bikerman model. A linear relationship between thickness and peel strength was observed and is consistent with the linearity of the Bikerman model. However, the Bikerman model greatly overestimated the strength (Figure 5). The Bikerman model predicts failure to occur when the stress at the crack tip exceeds the yield strength of the adhesive. This failure criterion may not apply to this material system. However, the overall shape of the predicted behavior (approximately linear decrease in peel strength with peel arm thickness) is similar to the observed behavior of

aluminum with varying thicknesses. This lends a degree of confidence in predicting the effect of peel arm thickness on overall peel strength.

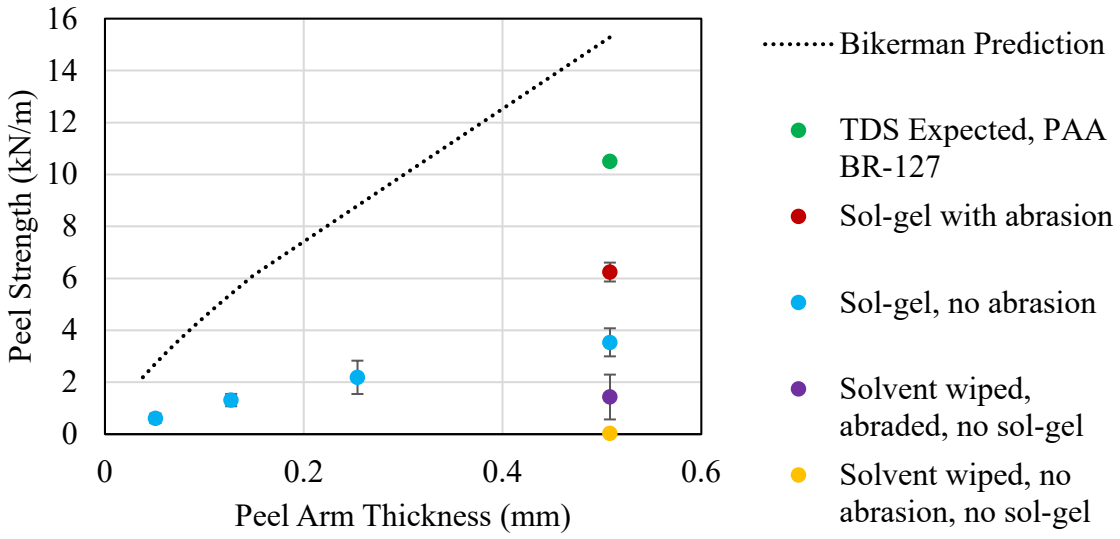

Figure 5. Relationship between peel strength and substrate thickness, as predicted through the Bikerman model and observed through testing on sol-gel coated aluminum.

3.5 Peel Strength of Amorphous Metal Foils

After demonstrating that sol-gel treatment generated peel strengths with aluminum substrates consistent with other work, and evaluating the effect of peel arm thickness on peel strength, these surface preparation methods were tested on the AM foils. Effect of sol-gel on the peel strength of MBF20 foils at the 0.05 and 0.08 mm (0.002 and 0.003 in) thicknesses was conducted. For initial testing, light abrasion was performed with care before sol-gel application, as abrasion before sol-gel is recommended by the manufacturer and provided the greatest peel strengths using aluminum substrates.

Failure mode was found to be cohesive in the adhesive, as confirmed both visually and with FTIR. Peel strength was found to increase 3- to 4-fold compared with solvent wiped only substrates, although the overall strength is low (Figure 6). This low strength does, however, correlate well with behavior observed with aluminum. This data suggests that the low peel strengths are governed by the mechanics of the peel test and not by the chemistry of the adhesive or surface treatment.

The 0.08 mm thick MBF20 exhibited higher peel strength compared with the 0.05 mm foil. This is likely due to the effect of substrate thickness on stress concentration at the peel front, as previously discussed. Additionally, the combination of abrasion and sol-gel appears to provide greater peel strengths compared with sol-gel without abrasion. This may indicate that abrasion or other surface treatment on the AM may be necessary to achieve improved peel strengths. For the application of JPL's Starshade assembly, abrasion may not be a practical step, and other surface activation techniques may be considered. Furthermore, since the failure mode is cohesive, further increasing the peel strength may only be achieved through exploration of additional surface treatments.

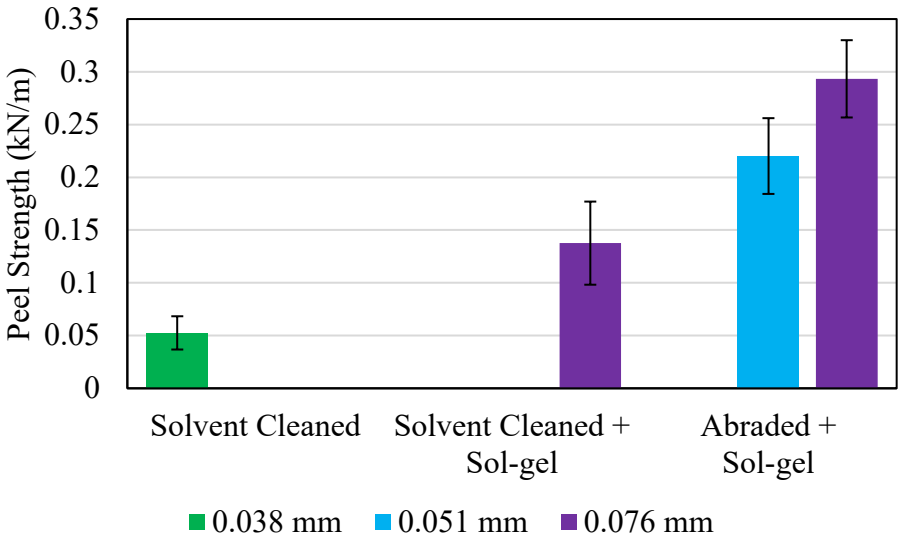

Figure 6. Peel strengths of MBF20 amorphous metal foil of three thicknesses, with and without abrasion and sol-gel. Error bars represent the standard deviation of at least four peel specimens. Note that these peel data were taken using a 200 lb load cell and greater noise at these strength values may be present.

4. CONCLUSIONS

Surface preparation methods for achieving TDS values for lap shear joints differ from those that will achieve a TDS value for peel strength joints. The addition of a primer was required for peel strength joints to approach similar forces to those reported in literature, which was lower than TDS peel strengths. The thickness of the flexible peel arm is the most likely cause of low peel strengths for amorphous foils. Additional peel strength can be achieved through the application of a primer and abraded surface, such as grit blasting and sol-gel AC-130. However, abrasion before applying a sol-gel coat may not be practical during the Starshade assembly and alternative surface activation techniques may be explored. Future research will explore additional coatings and surface treatments such as plasma polymerized silica to explore further peel strength improvements.

5. ACKNOWLEDGEMENTS

Portions of this research were funded through a subcontract with the Jet Propulsion Laboratory, California Institute of Technology, under a contract with the National Aeronautics and Space Administration.

6. REFERENCES

1. “Developing Starshade Technology to Image Earthsized Exoplaents around Neighboring Stars.” United States. National Aeronautics and Space Administration. 2017 Science Mission Directorate: Technology Highlights Washington, D.C.: GPO, 2017.
2. Steeves, John; Martin, Stefan; Webb, David; Lisman, Douglas; Shaklan, Stuart. “Precision Optical Edges for a Starshade External Occulter.” *Advances in Optical and Mechanical*

Technologies for Telescopes and Instrumentation II. Edinburgh, UK, 22 July 2016. Proc. SPIE 9912. Paper. DOI: 10.1117/12.2233409

3. Diegle, Ronald B. "Chemical Properties of Metallic Glasses." *Journal of Non-Crystalline Solids* 61&62 (1984): 601-612.
4. Jaray-Zadeh, M., Kumar, G. P., Branicio, P. S., Seifi, M., Lewandowski, J. J., and Cui, F. "A Critical Review on Metallic Glasses as Structural Materials for Cardiovascular Stent Applications." *Journal of Functional Biomaterials* 9(19) (2018). DOI:10.3390/jfb9010019
5. Our previous SAMPE paper
6. Abbott, Steven. Adhesion Science: Principles and Practice. Lancaster, Pennsylvania: DEStech Publications, Inc., 2015.
7. Li, Q.; Batra, R. C.; Graham, I.; Dillard, D. A. "Examining T-peel specimen bond length effects: Experimental and numerical explorations of transitions to steady-state debonding." *International Journal of Solids and Structures* 180-181 (2019): 72-83. DOI: 10.1016/j.ijsolstr.2019.07.012
8. Bikerman, J.J. "Theory of Peeling through a Hookean Solid." *Journal of Applied Physics* 28 (1957): 1484-1485. DOI: 10.1063/1.1722682
9. Kaelble, D. H. "Theory and Analysis of Peel Adhesion: Bond Stresses and Distributions." *Transactions of the Society of Rheology* 4 (1960): 45-73. DOI: 10.1122/1.548868
10. ASTM Standard D1002-10, "Apparent Shear Strength of Single-Lap-Joint Adhesively Bonded Metal Specimens by Tension Loading (Metal-to-Metal)" ASTM International, West Conshohocken, PA, 2019, DOI: 10.1520/D1002-10, www.astm.org.
11. "Technical Process Bulletin: Loctite EA 9394 Aero Epoxy Paste Adhesive." Henkel (2013).
12. "Technical Process Bulletin: Loctite EA 9360 Aero Epoxy Paste Adhesive." Henkel (2013).
13. ASTM Standard D3167-10, "Standard Test Method for Floating Roller Peel Resistance of Adhesives" ASTM International, West Conshohocken, PA, 2017, DOI: 10.1520/D3167-10R17, www.astm.org.
14. ASTM Standard E4-20, "Standard Practices for Force Verification of Testing Machines" ASTM International, West Conshohocken, PA, 2020, DOI:10.1520/E0004-20, www.astm.org.
15. Wisanrakkit, G. and Gillham, J. K. "Continuous heating transformation (CHT) cure diagram of an aromatic amine/epoxy system at constant heating rates." *Journal of Applied Polymer Science* 42(9) (1991): 2453-2463. DOI: 10.1002/app.1991.070420911
16. Hickey, C. M. D., and Bickerton, S. "Cure kinetics and rheology characterisation and modelling of ambient temperature curing epoxy resins for resin infusion/VARTM and wet layup applications." *Journal of Materials Science* 48 (2013): 690-701. DOI: 10.1007/s10853-012-6781-8
17. McCray, D. B., Smith, J. A., Storage, K. M., Ripberger, E. R., Shouse, M. D., and Mazza, J. J. "Nonmetallic Materials Supportability: The Evaluation of Two-Part Epoxy Paste Adhesives for Repair Bonding of Aluminum Alloys." *Air Force Research Laboratory Interim Report* (2011): AFRL-RX-WP-TR-2013-0054